

## Isolation and Characterization, Including by X-ray Crystallography, of Contact and Solvent-Separated Ion Pairs of Silenyl Lithium Species

Daniel Pinchuk, Jomon Mathew, Alexander Kaushansky, Dmitry Bravo-Zhivotovskii,\* and Yitzhak Apeloig\*

Dedicated to Professor Zvi Rappoport

**Abstract:** Reaction of bromoacysilane **1** (pink solution) with  $t\text{Bu}_2\text{MeSiLi}$  (3.5 equiv) in a 4:1 hexane:THF solvent mixture at  $-78^\circ\text{C}$  to room temperature yields the solvent separated ion pair (SSIP) of silenyl lithium  $E-[(t\text{BuMe}_2\text{Si})(t\text{Bu}_2\text{MeSi})\text{C}=\text{Si}(\text{SiMe}_2\text{Bu}_2)]^- [\text{Li}\cdot 4\text{THF}]^+$  **2a** (green–blue solution). Removal of the solvent and addition of benzene converts **2a** into the corresponding contact ion pair (CIP) **2b** (violet–red solution) with two THF molecules bonded to the lithium atom. The  $\mathbf{2a} \rightleftharpoons \mathbf{2b}$  interconversion is reversible upon  $\text{THF} \rightleftharpoons \text{benzene}$  solvent change. Both **2a** and **2b** were characterized by X-ray crystallography, NMR and UV/Vis spectroscopy, and theoretical calculations. The degree of dissociation of the Si–Li bond has a large effect on the visible spectrum (and thus color) and on the silenyl  $^{29}\text{Si}$  NMR chemical shift, but a small effect on the molecular structure. This is the first report of the X-ray molecular structure of both the SSIP and the CIP of any  $\text{R}_2\text{E}=\text{E}'\text{RM}$  species ( $\text{E} = \text{C}, \text{Si}; \text{E}' = \text{C}, \text{Si}; \text{M} = \text{metal}$ ).

Carbanions and other Group 14 anions are among the most important reagents in synthesis, and ion pairing plays an important role in dictating their chemistry.<sup>[1]</sup> It is therefore important to obtain information on their molecular structure, degree of aggregation and solvation, and their electronic structure. Ion pairing of organolithium compounds was studied extensively over the last decades, mostly by UV/Vis spectroscopy<sup>[1,2]</sup> and by NMR spectroscopy,<sup>[1,3]</sup> and important information collected.<sup>[1–3]</sup> However, there is relatively little information on the molecular structures and spectroscopic differences between the contact ion pairs (CIP) and the solvent-separated ion pairs (SSIP) of the same compound. X-ray structural data are only available for both the CIP and SSIP of the same compound for a few  $\text{R}_3\text{EM}$  systems ( $\text{E} = \text{Group 14 element}; \text{M} = \text{alkali metal}$ ); for example,  $\text{Ph}_3\text{CLi}$ ,<sup>[4]</sup>  $(\text{Me}_3\text{Si})_3\text{SiK}$ ,<sup>[5]</sup>  $(t\text{Bu}_2\text{MeSi})_3\text{SiLi}$ ,<sup>[6]</sup> and  $(t\text{Bu}_2\text{MeSi})_3\text{SnLi}$ .<sup>[7]</sup> In contrast, in the case of  $\text{R}_2\text{E}=\text{E}'\text{RM}$  ( $\text{E} = \text{C}, \text{Si}; \text{E}' = \text{C}, \text{Si}$ ;

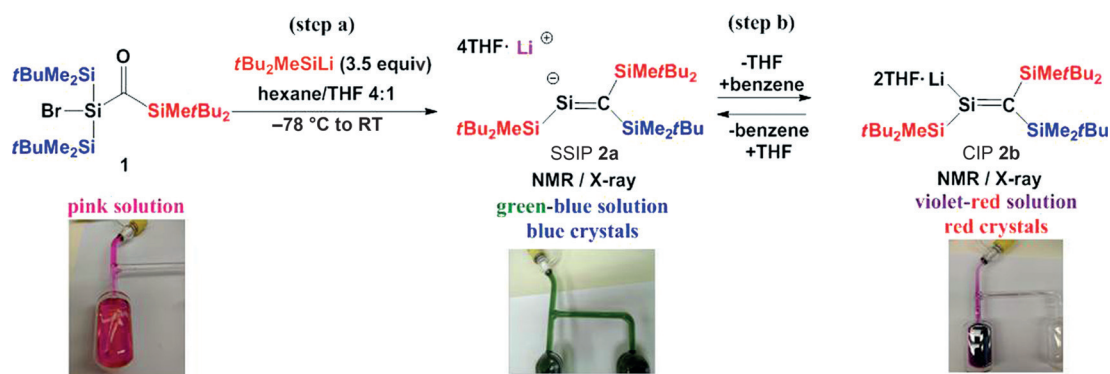
$\text{M} = \text{metal}$ ) structural data for both ion pair types is not available. We note that  $\text{R}_2\text{E}=\text{E}'\text{RM}$  compounds (where  $\text{E}, \text{E}' = \text{Ge}, \text{Sn}$ ) are not yet known.

In recent years, there is a growing interest in the chemistry of organosilicon compounds in general,<sup>[8]</sup> and in alkali-metal silanes (silyl anions) as important potential synthetic building blocks in particular.<sup>[9,10]</sup> Recently, several disilenyl anions (disilenides)  $\text{R}_2\text{Si}=\text{SiRM}$  ( $\text{M} = \text{Li}, \text{Na}, \text{K}$ ), the silicon analogues of vinyl anions, were synthesized<sup>[10]</sup> and their synthetic applications are being explored.<sup>[9,10]</sup> Several disilenides were characterized by X-ray crystallography, all as CIP,<sup>[10]</sup> but the corresponding SSIP were not isolated. Both the CIP and the SSIP were only isolated for one disilenyl lithium species: the structure of the CIP was determined by X-ray crystallography, but attempts to determine the X-ray structure of the corresponding SSIP failed.<sup>[10a]</sup> In two other cases the SSIP of a disilenyl lithium were isolated,<sup>[11]</sup> but the corresponding CIP was not reported. We recently reported the synthesis of the first silenyl lithiums,  $E-(1\text{-Ad})-(t\text{Bu}_2\text{MeSi})\text{C}=\text{SiRLi}\cdot 2\text{THF}$  ( $\text{R} = \text{SiMe}_2\text{Bu}_2$  (**3**);  $\text{R} = \text{SiMe}_2t\text{Bu}$  (**3a**)),<sup>[12]</sup> which were characterized by X-ray crystallography as a CIP; the corresponding SSIP is not known. Herein, we report the synthesis, X-ray crystallography molecular structures, and the UV/Vis and NMR spectra of both the SSIP (or fully dissociated) **2a** and the corresponding CIP **2b** of a novel persilyl silenyl lithium (Scheme 1). **2a** and **2b** reversibly interconvert by a  $\text{THF} \rightleftharpoons \text{benzene}$  solvent change, exhibiting a spectacular color change from green–blue (**2a**) to violet–red (**2b**). To our best knowledge, the effect of dissociation of a CIP to a SSIP on the molecular structure and the UV/Vis and NMR spectra of any  $\text{R}_2\text{E}=\text{E}'\text{RM}$  (namely, vinyl lithiums,<sup>[3a,b,13]</sup> silenyl lithiums,<sup>[12]</sup> or disilenyl lithiums<sup>[9a,10]</sup>) has not been reported previously.

The SSIP and CIP persilyl silenyl lithiums **2a** and **2b** were synthesized in a manner similar to the previously reported 1-adamantyl substituted silenyl lithium  $E-(1\text{-Ad})-(t\text{Bu}_2\text{MeSi})\text{C}=\text{Si}(\text{SiMe}_2\text{Bu}_2)\text{Li}\cdot 2\text{THF}$  (**3**),<sup>[12]</sup> by a one-pot reaction of the pink 4:1 hexane:THF solution of bromoacysilane **1** with  $t\text{Bu}_2\text{MeSiLi}$  (3.5 equiv) at  $-78^\circ\text{C}$ ,<sup>[14]</sup> followed by warming to room temperature over 2 h. The reaction yields a green–blue solution of **2a** in 80% yield (Scheme 1, step a).<sup>[15]</sup> Removal of the solvent and crystallization from THF yields blue crystals, determined by X-ray crystallography to be the SSIP silenyl anion weakly interacting with a  $[\text{Li}\cdot 4\text{THF}]^+$  cation (**2a**), with an  $r(\text{Si}\text{--}\text{Li})$  of 7.17 Å. Upon evaporation of the hexane:THF solvent from the green–blue

[\*] D. Pinchuk, Dr. J. Mathew, A. Kaushansky, Dr. D. Bravo-Zhivotovskii, Prof. Dr. Y. Apeloig  
Schulich Faculty of Chemistry and the Lise Meitner-Minerva Center for Computational Quantum Chemistry  
Technion-Israel Institute of Technology  
Haifa 32000 (Israel)  
E-mail: chrbrzh@tx.technion.ac.il  
apeloig@technion.ac.il

Supporting information and the ORCID identification number(s) for the author(s) of this article can be found under <http://dx.doi.org/10.1002/anie.201603640>.



**Scheme 1.** Synthesis of silenyl lithiums SSIP **2a** and CIP **2b**.

solution of **2a** and addition of benzene, the solution turns violet–red. Crystallization from benzene at room temperature yields red crystals determined by X-ray crystallography to be the CIP silenyl lithium, with the lithium atom coordinated to two THF molecules (**2b**) with an  $r(\text{Si-Li})$  of 2.713(12) Å (Scheme 1, step b). Natural Bond Orbital (NBO)<sup>[16]</sup> analysis of **2b** predicts a highly polarized Si–Li bond. That is, 92 % and 8 % of the  $\sigma(\text{Si-Li})$  electron density resides on the silicon and lithium atoms, respectively.<sup>[14]</sup> Natural Resonance Theory (NRT)<sup>[17]</sup> analysis of a model system  $(\text{Me}_3\text{Si})_2\text{C}=\text{Si}(\text{SiMe}_3)\text{Li}\cdot 2\text{THF}$  predicts a Si–Li natural bond order of 0.91 with an ionic contribution of 0.79 and a covalent contribution of 0.12, pointing to a high ionic character of the Si–Li bond.

Evaporation of the benzene solvent from a **2b** solution and addition of THF yields **2a** (green–blue solution). Addition of benzene to blue crystals of **2a** effectively removes two THF molecules, yielding only CIP **2b** in benzene solution. Thus, in benzene solvent it is not possible to observe **2a**. The SSIP **2a**⇌CIP **2b** transformation is reversible and controlled by THF⇌benzene solvent change. This is a unique example of a CIP⇌SSIP reversible interconversion by solvent change of a  $\text{R}_2\text{E}=\text{E}'\text{RM}$  system, where both species were isolated and characterized by X-ray crystallography.

The visible spectrum of SSIP **2a** in THF shows a wide absorption with a peak at  $\lambda = 585 \text{ nm}$  ( $\epsilon = 150 \text{ M}^{-1} \text{ cm}^{-1}$ )

red-shifted by 59 nm relative to that of CIP **2b** in benzene ( $\lambda = 526 \text{ nm}$ ,  $\epsilon = 225 \text{ M}^{-1} \text{ cm}^{-1}$ ; Figure 1).<sup>[14]</sup> These absorptions correspond to the observed green–blue (**2a**) and violet–red (**2b**) solution colors.

The UV/Vis spectra of **2a''** (free anion of **2a**) and **2b** were calculated using TD-DFT theory<sup>[18]</sup> at the PBE0<sup>[19]</sup>/6-31 + G(d,p)//B97D<sup>[20]</sup>/6-31 + G(d,p) level of theory.<sup>[14]</sup> Solvent effects were calculated by the Polarizable Continuum Model (PCM)<sup>[21]</sup> for **2a''** in THF and for **2b** in benzene. These calculations predict absorptions at 562 nm (**2a''**) and 505 nm (**2b**), somewhat shifted from the experimental values, but the calculated **2b**→**2a''** red-shift of 57 nm is in excellent agreement with the experimental (59 nm). The observed 585 nm (**2a**) and 526 nm (**2b**) absorptions are attributed to a forbidden HOMO→LUMO transition, in agreement with the observed low  $\epsilon$  values. In both species the HOMO is the in-plane  $\sigma$  ( $\text{sp}^2$ -type) anionic lone pair orbital on the silenyl atom and the LUMO is the  $\pi^*(\text{C}=\text{Si})$  orbital (Figure 1). The  $\pi(\text{C}=\text{Si})$  orbital is the HOMO-1 orbital in both **2a''** and **2b**.<sup>[22]</sup> The calculated HOMO→LUMO ( $\sigma \rightarrow \pi^*$ ) energy gap of 3.64 eV in **2b** is larger than that in **2a''** (3.38 eV), explaining the observed red-shift for the CIP **2b**→SSIP **2a** transformation (Figure 1). The **2b**→**2a''** red-shift is due to an increase of 1.16 eV in the HOMO energy of **2a''** relative to **2b**, which is partially offset by the 0.9 eV higher LUMO energy of **2a''** versus that of **2b** (Figure 1). The calculated HOMO→LUMO

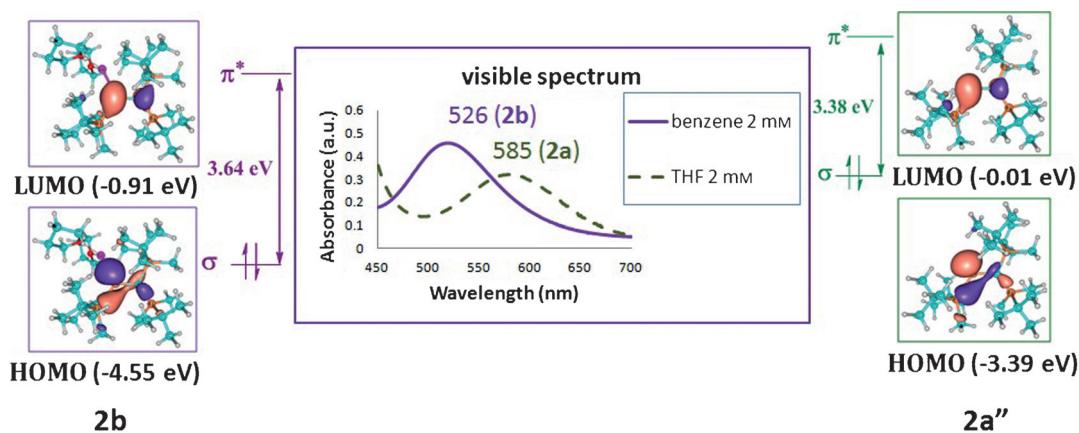


**Figure 1.** Experimental visible spectra of **2a** and **2b** and the calculated frontier molecular orbitals of **2a''** (free anion of **2a**) and **2b**.

( $\sigma \rightarrow \pi^*$ ) energy gap in **3** of 3.96 eV is in line with its calculated absorption maximum at 447 nm.

The NMR spectra of **2a** and **2b** provide interesting information. The chemical shift of the silenilic Si<sup>1</sup> is 347.8 ppm in CIP **2b** (Table 1)<sup>[23,24]</sup> and it is downfield shifted by 57.7 ppm to 405.5 ppm in SSIP **2a**. Tentatively, it is expected that  $\delta(^{29}\text{Si}^1)$  in **2a** would be upfield shifted relative to **2b**, as the formal negative charge on the silenyl unit in dissociated **2a** is higher than that in Si–Li bonded **2b**. The observed **2b**  $\rightarrow$  **2a** downfield shift also contrasts with the data of other silyllithiums; for example,  $\delta(^{29}\text{Si}^1) = -185$  ppm in CIP (*t*Bu<sub>2</sub>MeSi)<sub>3</sub>SiLi, and  $-195$  ppm in SSIP (*t*Bu<sub>2</sub>MeSi)<sub>3</sub>Si<sup>−</sup>[Li·4THF]<sup>+</sup>.<sup>[25]</sup> Substituting the silyl group at the vinylic C<sup>1</sup> in **2b** for a 1-adamantyl substituent (that is, **3**) results in a significant upfield shift of  $\delta(\text{Si}^1)$  to 241.8 ppm.<sup>[12]</sup> This is in line with the general observed trend that more electro-negative substituents (for example, alkyl vs. silyl) shift the <sup>29</sup>Si NMR resonances of disilenes upfield.<sup>[9a]</sup>  $\delta(^{13}\text{C}^1)$  is at 143.8 and 134.1 ppm in **2b** and **2a**, respectively, which is shielded compared to **3** (175.2 ppm). The chemical shift of <sup>7</sup>Li ( $-0.41$  ppm (**2b**) and  $-0.31$  ppm (**2a**)), is only slightly affected by the degree of dissociation of the Si–Li bond.<sup>[23]</sup>

To obtain insight into these unusual NMR chemical shift changes, the chemical shifts of **2a'**, **2b**, and **3** were calculated at the HCTH407<sup>[26]</sup>/def2-TZVPP<sup>[27]</sup>//B97D/6-31 + G(d,p) level of theory (Table 1; Supporting Information). The calculated  $\delta(^{29}\text{Si}^1)$ , and in particular the changes in  $\delta(^{29}\text{Si}^1)$  between these molecules, are in very good agreement with the experimental (Table 1). To better understand the surprising downfield shift of  $\delta(^{29}\text{Si}^1)$  in **2a** compared to **2b** the calculated total isotropic chemical shielding values ( $\sigma_{\text{iso}}$ ) were separated into contributions from the diamagnetic ( $\sigma_{\text{d}}$ ) and the paramagnetic ( $\sigma_{\text{p}}$ ) chemical shielding. The latter results from paramagnetic currents induced by the applied magnetic field, which couples occupied and virtual orbitals, causing a downfield shift (deshielding). The computational results (Table 1), show that  $\sigma(^{29}\text{Si}^1_{\text{iso}})_{\text{p}}$  of the free silenyl anion **2a'** is downfield shifted by 45.1 ppm relative to that of CIP **2b**, close to the 57.1 ppm downfield shift of  $\delta(^{29}\text{Si}^1)_{\text{iso}}$ , indicating that  $\delta(^{29}\text{Si}^1)$  is dictated by the paramagnetic component. The **2b**  $\rightarrow$  **3** substitution leads to a calculated upfield shift in  $\sigma(^{29}\text{Si}^1_{\text{iso}})_{\text{p}}$  of 92.6 ppm (Table 1), almost equivalent to the calculated and experimental upfield shift of 100.6 ppm exhibited by  $\delta(^{29}\text{Si}^1)_{\text{iso}}$  (Table 1). According to the Ramsey equation,<sup>[28]</sup> the paramagnetic component of the chemical shielding is inversely proportional to the sum of the energy differences between the orbitals coupled by the applied magnetic field. For **2a** and **2b**

the HOMO–LUMO coupling has the largest effect on the <sup>29</sup>Si<sup>1</sup> paramagnetic tensor components.<sup>[29]</sup> Thus, the observed **2b**  $\rightarrow$  **2a** downfield shift of  $\delta(^{29}\text{Si}^1)_{\text{iso}}$  (Table 1) can be attributed to the smaller  $\Delta E(\text{HOMO}–\text{LUMO})$  in **2a** ( $-3.38$  eV) than that in **2b** ( $-3.64$  eV; Table 1). Alkyl versus silyl substitution at C<sup>1</sup> (**3**) increases  $\Delta E(\text{HOMO}–\text{LUMO})$  to  $-3.96$  eV, causing an upfield shift in  $\delta(^{29}\text{Si}^1)_{\text{iso}}$ . These computational results nicely explain the counterintuitive behavior of the measured  $\delta(^{29}\text{Si}^1)$  NMR chemical shifts of **2a** versus **2b**. The effect of the counteraction on the Si–M bonding was also studied. The calculated  $\delta(^{29}\text{Si}^1)$  in (Me<sub>2</sub>*t*BuSi)(*t*Bu<sub>2</sub>MeSi)C=Si<sup>1</sup>(SiMe*t*Bu<sub>2</sub>)K·2THF is 373.6 ppm, downfield shifted by 22.5 ppm relative to **2b**, as expected. This observation points to a higher ionic character in the potassium than in the lithium compound.

The X-ray molecular structure of CIP **2b**, where the lithium atom is coordinated to two THF molecules, shows that the Si–Li distance is 2.713(12) Å (Figure 2),<sup>[30]</sup> longer than in CIP **3·2THF** 2.613(6) Å, shorter than that in CIP Tip<sub>2</sub>Si=Si(Tip)Li·2THF 2.853(3) Å (Tip = 2,4,6-*i*Pr<sub>3</sub>C<sub>6</sub>H<sub>2</sub>),<sup>[10a]</sup> but longer than in CIP (*t*Bu<sub>2</sub>MeSi)<sub>2</sub>Si=Si(SiMe*t*Bu<sub>2</sub>)Li·2THF (2.598(9) Å).<sup>[9b]</sup> The *r*(Si–Li) range in these very similar compounds is large (0.255 Å), indicating the lability of the Si–Li bond.

The crystals of **2a**, in which the lithium atom is complexed by four THF molecules, are of relatively low quality (*R* = 11.56 %), but the X-ray crystallographic analysis clearly shows that **2a** has a very long Si–Li distance of 7.17 Å,<sup>[30]</sup> that is, with no covalent Si–Li bonding. **2a** is therefore characterized as a solvent separated (or fully dissociated) silenyl anion, loosely interacting with the [Li·4THF]<sup>+</sup> counteraction. Better quality crystals (*R* = 8.92 %) are obtained by reacting **2b** in benzene with one equivalent of 12-crown-4, yielding blue crystals of **2c** (**2c** is insoluble in benzene) in which Li<sup>+</sup> is chelated by both 12-crown-4 and THF, and the Si–Li distance is 7.223(1) Å (Figure 3).<sup>[30]</sup>

Table 2 compares the most important bond lengths and bond angles of CIP **2b** and SSIP **2c**. There are only minor structural differences in the silenyl unit between the CIP **2b** and SSIP **2c**.<sup>[14,30]</sup> This is surprising considering that in **2c** there is a significantly higher NBO negative charge on the silenyl unit ( $-1$  el.) than in **2b** ( $-0.72$  el.). The C=Si bond length in **2c** and **2b** is nearly the same (1.766(3) Å vs. 1.762(3) Å, respectively), similar to that in **3** (1.773(3) Å)<sup>[12]</sup> and in (Me<sub>3</sub>Si)<sub>2</sub>Si=C(1-Ad)(OSiMe<sub>3</sub>) (1.764(3) Å),<sup>[31]</sup> but longer than in (*t*BuMe<sub>2</sub>Si)(Me<sub>3</sub>Si)Si=Ad (1.741(2) Å)<sup>[32]</sup> and in Me<sub>2</sub>Si=C(SiMe<sub>3</sub>)(SiMe*t*Bu<sub>2</sub>) (1.702(3) Å).<sup>[33]</sup> The geometry

**Table 1:** Experimental and calculated <sup>29</sup>Si<sup>1</sup>, <sup>13</sup>C<sup>1</sup>, and <sup>7</sup>Li chemical shifts, the calculated <sup>29</sup>Si NMR isotropic shielding ( $\sigma_{\text{iso}}$ ), the isotropic paramagnetic shielding component ( $\sigma_{\text{p}}$  (ppm)), and  $\Delta E(\text{HOMO}–\text{LUMO})$  of **2a**, **2b**, and **3**.

Compound	$\delta(^{29}\text{Si}^1)$		$\sigma(^{29}\text{Si}^1)_{\text{iso}}$		$\delta(^{13}\text{C}^1)$		$\delta(^7\text{Li})$	
	exp.	calc. <sup>[a]</sup>	calc. <sup>[a]</sup>	calc. <sup>[a]</sup>	exp.	calc. <sup>[a]</sup>	exp.	calc. <sup>[a]</sup>
<b>2a</b>	405.5	408.2 <sup>[d]</sup>	$-80.7^{\text{[d]}}$	$-986.2^{\text{[d]}}$	134.1	141.6 <sup>[d]</sup>	$-0.31$	$-3.38^{\text{[d]}}$
<b>2b</b>	347.8	351.1	$-23.6$	$-941.1$	143.8	160.2	$-0.41$	$-3.64$
<b>3</b>	241.8	250.5	$77.0$	$-848.5$	175.2	191.6	–	$-3.96$
$\Delta(\mathbf{2a}–\mathbf{2b})$	57.7	57.1	$57.1^{\text{[d]}}$	$45.1^{\text{[d]}}$	9.7	$18.6^{\text{[d]}}$	0.10	$0.26^{\text{[d]}}$
$\Delta(\mathbf{2b}–\mathbf{3})$	106.0	100.6	100.6	92.6	31.4	31.4	–	0.32

[a] At HCTH407/def2-TZVPP//B97D/6-31 + G(d,p); [b]  $\Delta E$  (HOMO–LUMO) in eV; [c] at PBE0/6-31 + G(d,p) // B97D/6-31 + G(d,p) (using PCM: **2a'** in THF, **2b**, and **3** in benzene); [d] for **2a'**.



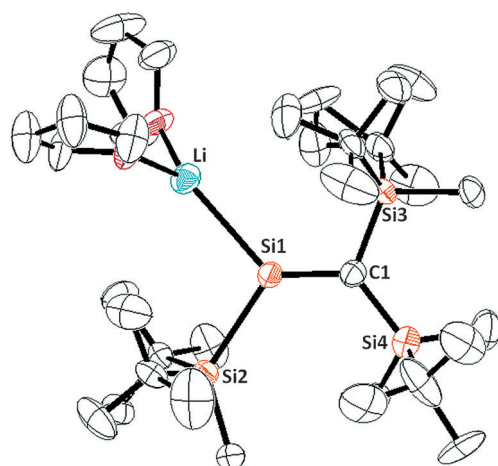


**Figure 2.** ORTEP drawing of the X-ray molecular structure of CIP **2b**. Hydrogen atoms were omitted for clarity and the thermal ellipsoids are set at the 75 % probability level. Selected geometrical parameters are given in Table 2.<sup>[30]</sup> and the full details are given in CCDC 1473316 and the Supporting Information.

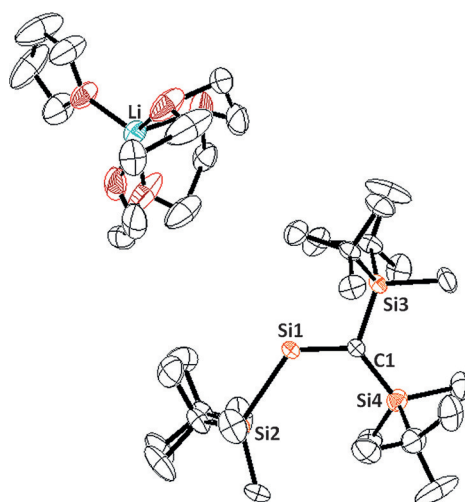


**Figure 3.** ORTEP drawing of the X-ray molecular structure of **2c**. The hydrogen atoms were omitted for clarity, and the thermal ellipsoids are set at the 75 % probability level. Selected geometrical parameters are given in Table 2.<sup>[30]</sup> and the full details are given in CCDC 1473317 and the Supporting Information.

**Table 2:** Experimental and calculated<sup>[a]</sup> main geometric parameters of **2b**, **2c**, **2a''**, and **3**.

Compound	Method	Si–Li	C=Si	Si <sup>1</sup> –Si <sup>2</sup>	∠C <sup>1</sup> Si <sup>1</sup> Si <sup>2</sup>	∠Si <sup>4</sup> C <sup>1</sup> Si <sup>1</sup> Si <sup>2</sup>
<b>2b</b>	exp.	2.713(12)	1.762(3)	2.486(2)	124.1(2)	5.0(3)
<b>2b</b>	calc.	2.616	1.795	2.416	124.3	11.3
<b>2c</b>	exp.	7.223(1)	1.766(3)	2.443(5)	125.1(7)	6.3(8)
<b>2a''</b>	calc.	–	1.811	2.458	121.02	0.38
<b>3</b>	exp.	2.613(6)	1.773(3)	2.408(11)	123.7(9)	6.0(1) <sup>[b]</sup>
<b>3</b>	calc.	2.580	1.799	2.397	122.86	3.3 <sup>[b]</sup>

[a] At B97D/6-31 + G(d,p); [b]  $\angle C(1-Ad)-C^1 = Si^1-Si^2$ .

around the C=Si bond is nearly planar in both **2b** and **2c**, that is, no pyramidalization at C<sup>1</sup> ( $\Sigma\theta = 359.8^\circ$  in both **2b** and **2c**) or Si<sup>1</sup> ( $\Sigma\theta = 359.8^\circ$  in **2b**), and there is only a slight twisting around the C=Si bond;  $\angle Si^4C^1Si^1Si^2$  is  $5.0^\circ$  in **2b** and  $6.3^\circ$  in **2c**. The Si<sup>1</sup>–Si<sup>2</sup> distance in **2c** (2.443(5) Å) is shorter by 0.043 Å than in **2b** (2.486(2) Å). As expected for an sp<sup>2</sup>-type anion, **2c** and **2b** are strongly bent;  $\angle C^1Si^1Si^2$  is  $125.1^\circ$  in **2c** and  $124.1^\circ$  in **2b**. The DFT calculated structures of **2b** and of the corresponding free silenyl anion **2a''** are in good agreement with the experimental (Table 2).<sup>[30]</sup>

In conclusion, we report the X-ray crystallographic structures, UV/Vis spectra, and NMR chemical shifts of both contact (**2b**) and solvent separated ion pairs (**2a** and **2c**) of a novel silenyl lithium (relevant data<sup>[14]</sup> is provided in the Supporting Information). **2a** and **2b** can be interconverted by a THF⇌benzene solvent change. This is the first example of a reversible interconversion of CIP⇌SSIP by solvent change for any R<sub>2</sub>E=E'RM (E = C, Si; E' = C, Si; M = metal), where both species are characterized by X-ray crystallography. While the molecular structure is only slightly affected by dissociation (that is, **2b**→**2c**) the solution color changes from violet–red (**2b**) to green–blue (**2a**, **2c**), and the silenyl <sup>29</sup>Si NMR chemical shift is shifted downfield significantly. We are currently studying the reactions of this novel silenyl lithium.

## Acknowledgements

This research was supported by the Israel Science Foundation (ISF), the Deutsch-Israelische Projektkooperation (DIP), and the Minerva Foundation in Munich. D.B.-Z. is grateful to Israel's Ministry of Immigrant Absorption, for a Kamea fellowship. We thank Dr. M. Karni for helpful discussions.

**Keywords:** bis(silyl)ketone · ion pairs · lithium · low-valent compounds · silicon

**How to cite:** *Angew. Chem. Int. Ed.* **2016**, 55, 10258–10262  
*Angew. Chem.* **2016**, 128, 10414–10418

- [1] a) H. J. Reich, *Chem. Rev.* **2013**, 113, 7130–7178; b) G. Fraenkel in *The Chemistry of Organolithium Compounds*, Vol. 2 (Eds.: Z. Rappoport, I. Marek), Wiley-VCH, Weinheim, **2004**, pp. 1–63.
- [2] a) E. Buncel, B. Menon, *J. Org. Chem.* **1979**, 44, 317–320; b) J. Smid, *Angew. Chem. Int. Ed. Engl.* **1972**, 11, 112–127; *Angew. Chem.* **1972**, 84, 127–144.
- [3] a) R. Knorr, K.-O. Hennig, P. Böhler, B. Schubert, *J. Organomet. Chem.* **2014**, 767, 125–135; b) R. Knorr, T. Menke, C. Behringer, K. Ferchland, J. Mehlstäubel, E. Lattke, *Organometallics* **2013**, 32, 4070–4081; c) P. R. Carlier, C. W. S. Lo, *J. Am. Chem. Soc.* **2000**, 122, 12819–12823; d) H. J. Reich, R. R. Dykstra, *J. Am. Chem. Soc.* **1993**, 115, 7041–7042; e) A. T. Weibel, J. P. Oliver, *J. Organomet. Chem.* **1974**, 82, 281–290.

- [4] a) M. M. Olmstead, P. P. Power, *J. Am. Chem. Soc.* **1985**, *107*, 2174–2175; b) J. J. Brooks, G. D. Stucky, *J. Am. Chem. Soc.* **1972**, *94*, 7333–7338.
- [5] D. M. Jenkins, W. Teng, U. Englich, D. Stone, K. Ruhlandt-Senge, *Organometallics* **2001**, *20*, 4600–4606.
- [6] A. Sekiguchi, T. Fukawa, M. Nakamoto, V. Y. Lee, M. Ichinohe, *J. Am. Chem. Soc.* **2002**, *124*, 9865–9869.
- [7] T. Fukawa, M. Nakamoto, V. Y. Lee, A. Sekiguchi, *Organometallics* **2004**, *23*, 2376–2381.
- [8] a) V. Y. Lee, A. Sekiguchi, *Organometallic Compounds of Low-Coordinate Si, Ge, Sn and Pb: From Phantom Species to Stable Compounds*, Wiley, Chichester, **2010**; b) M. A. Brook, *Silicon in Organic Organometallic, and Polymer Chemistry*, Wiley-VCH, Weinheim, **2000**; c) *The Chemistry of Organic Silicon Compounds*, Vol. 2, 3, *Parts 1–3*, (Eds.: Z. Rappoport, Y. Apeloig), Wiley, New York, **1998**, **2001**.
- [9] a) D. Scheschkewitz, *Chem. Lett.* **2011**, *40*, 2–11; b) R. C. Fischer, P. P. Power, *Chem. Rev.* **2010**, *110*, 3877–3923; c) D. Scheschkewitz, *Chem. Eur. J.* **2009**, *15*, 2476–2485; d) M. Nanjo, A. Sekiguchi in *Silicon-Containing Dendritic Polymers* (Eds.: P. R. Dvornic, M. J. Owen), Springer, Amsterdam, **2009**, Chapter 4; e) H.-W. Lerner, *Coord. Chem. Rev.* **2005**, *249*, 781–798; f) A. Sekiguchi, V. Y. Lee, M. Nanjo, *Coord. Chem. Rev.* **2000**, *210*, 11–45.
- [10] a) D. Scheschkewitz, *Angew. Chem. Int. Ed.* **2004**, *43*, 2965–2967; *Angew. Chem.* **2004**, *116*, 3025–3028; b) M. Ichinohe, K. Sanuki, S. Inoue, A. Sekiguchi, *Organometallics* **2004**, *23*, 3088–3090; c) S. Inoue, M. Ichinohe, A. Sekiguchi, *Chem. Lett.* **2005**, *34*, 1564–1565; d) M. Ichinohe, K. Sanuki, S. Inoue, A. Sekiguchi, *Silicon Chem.* **2007**, *3*, 111–116; e) T. Iwamoto, M. Kobayashi, K. Uchiyama, S. Sasaki, S. Nagendran, H. Isobe, M. Kira, *J. Am. Chem. Soc.* **2009**, *131*, 3156–3157.
- [11] a) H. Yasuda, V. Y. Lee, A. Sekiguchi, *J. Am. Chem. Soc.* **2009**, *131*, 6352–6353; b) R. Kinjo, M. Ichinohe, A. Sekiguchi, *J. Am. Chem. Soc.* **2007**, *129*, 26–27.
- [12] L. Zborovsky, R. Dobrovetsky, M. Botoshansky, D. Bravo-Zhivotovskii, Y. Apeloig, *J. Am. Chem. Soc.* **2012**, *134*, 18229–18232.
- [13] W. Bauer, C. Griesinger, *J. Am. Chem. Soc.* **1993**, *115*, 10871–10882.
- [14] For details see the Supporting Information: the synthesis and spectroscopic data of **1**, **2a**, **2b**, and **2c**; X-ray crystallographic data for **2a**, **2b**, and **2c**; calculated optimized geometries, NMR chemical shifts, and UV/Vis spectra of **2b**, **2a''**, and **3**; and Natural Chemical Shielding (NCS) calculations for model systems  $(\text{H}_3\text{Si})_2\text{C}=\text{Si}(\text{SiH}_3)^-$ ,  $(\text{H}_3\text{Si})_2\text{C}=\text{Si}(\text{SiH}_3)\text{Li}\cdot 2\text{THF}$ ,  $(\text{H}_3\text{C})(\text{H}_3\text{Si})\text{C}=\text{Si}(\text{SiH}_3)^-$  and  $(\text{H}_3\text{C})(\text{H}_3\text{Si})\text{C}=\text{Si}(\text{SiH}_3)\text{Li}\cdot 2\text{THF}$ .
- [15] The reaction probably proceeds via the corresponding silenolate  $E^-[(t\text{BuMe}_2\text{Si})_2\text{Si}=\text{C}(\text{OLi})(\text{SiMe}_2\text{Bu}_2)]$ , which was not isolated. See the Supporting Information and Lit. [12].
- [16] A. E. Reed, R. B. Weinstock, F. Weinhold, *J. Chem. Phys.* **1985**, *83*, 735–746.
- [17] a) E. D. Glendening, F. Weinhold, *J. Comput. Chem.* **1998**, *19*, 593–609; b) E. D. Glendening, F. Weinhold, *J. Comput. Chem.* **1998**, *19*, 610–627; c) E. D. Glendening, J. K. Badenhop, F. Weinhold, *J. Comput. Chem.* **1998**, *19*, 628–646.
- [18] Gaussian 09 (Revision D.01), M. J. Frisch, et al., Gaussian, Inc., Wallingford CT, **2010** was used; for the full list of authors see the Supporting Information.
- [19] a) C. Adamo, V. Barone, *J. Chem. Phys.* **1999**, *110*, 6158–6170; b) J. P. Perdew, K. Burke, M. Ernzerhof, *Phys. Rev. Lett.* **1996**, *77*, 3865–3868.
- [20] S. Grimme, *J. Comput. Chem.* **2006**, *27*, 1787–1799.
- [21] a) J. Tomasi, B. Mennucci, R. Cammi, *Chem. Rev.* **2005**, *105*, 2999–3093; b) G. Scalmani, M. J. Frisch, B. Mennucci, J. Tomasi, R. Cammi, V. Barone, *J. Chem. Phys.* **2006**, *124*, 1–15.
- [22] Based on the visual similarity of the frontier molecular orbitals of **2a** and those of a silylene,  $\text{R}_2\text{Si}$  (both have a  $\sigma$ -lone pair and low-lying empty  $p/\pi$ -type orbital), one of the referees suggested that **2a** has a partial contribution of a silylene-type resonance structure. We examined this interesting suggestion and computationally studied a close silylene model to **2a**, that is,  $(\text{Me}_2\text{rBuSi})(t\text{Bu}_2\text{MeSi})(\text{H})\text{C}^1\text{-Si}^1(\text{SiMe}_2\text{Bu}_2)$  (**2d**). The calculations reveal very large differences between **2d** and **2a''** (free anion of **2a**). Thus, the  $\text{C}^1\text{-Si}^1$  bond length in **2d** is 0.134 Å longer than that in **2a''** (1.945 Å vs. 1.811 Å, respectively). Furthermore,  $\delta(^{29}\text{Si}^1)$  in **2d** is downfield shifted by 362 ppm relative to **2a''** (770.2 vs. 408.2 ppm, respectively). The calculated visible spectrum of **2d** is red-shifted by 97 nm relative to that of **2a''** ( $\lambda = 659$  vs.  $\lambda = 562$  nm, respectively). These large differences in the NMR chemical shifts, visible absorptions, and  $r(\text{Si}=\text{C})$  between **2d** versus **2a''** clearly indicate that the contribution of a silylene-type resonance structure toSSIP **2a**, if any, is minor.
- [23] The observed broadening of the 347.8 ppm signal (see the Supporting Information) might arise from coupling of the silicon atom to the coordinated  $^7\text{Li}$  nucleus. However, quartet splitting of the  $^{29}\text{Si}$  NMR signal was not observed. Unfortunately we cannot measure the  $^{29}\text{Si}\text{-}^6\text{Li}$  coupling constant ( $J$ ).
- [24] For comparison of CIP  $\delta(^{29}\text{Si}^1)$  values:  $(t\text{Bu}_2\text{MeSi})_2\text{Si}=\text{Si}(\text{SiMe}_2\text{Bu}_2)\text{Li}\cdot 2\text{THF}$  resonates at 328.4 ppm<sup>[10c]</sup> and  $\text{Tip}_2\text{Si}=\text{Si}(\text{Tip})\text{Li}\cdot 2\text{THF}$  at 100.5 ppm<sup>[10a]</sup>.
- [25] M. Nakamoto, T. Fukawa, V. Y. Lee, A. Sekiguchi, *J. Am. Chem. Soc.* **2002**, *124*, 15160–15161.
- [26] A. D. Boese, N. C. Handy, *J. Chem. Phys.* **2001**, *114*, 5497–5503.
- [27] a) F. Weigend, *Phys. Chem. Chem. Phys.* **2006**, *8*, 1057–1065; b) F. Weigend, R. Ahlrichs, *Phys. Chem. Chem. Phys.* **2005**, *7*, 3297–3305.
- [28] a) *Molecular Quantum Mechanics*, 3rd ed.; P. W. Atkins, R. S. Friedman, Eds.; Oxford University Press: Oxford, U. K., **1997**; b) N. F. Ramsey, *Phys. Rev.* **1950**, *78*, 695–699.
- [29] a) Based on Natural Chemical Shielding (NCS)<sup>[29b]</sup> calculations of the model systems  $(\text{H}_3\text{Si})_2\text{C}=\text{Si}(\text{SiH}_3)^-$ ,  $(\text{H}_3\text{Si})_2\text{C}=\text{Si}(\text{SiH}_3)\text{Li}\cdot 2\text{THF}$ ,  $(\text{H}_3\text{C})(\text{H}_3\text{Si})\text{C}=\text{Si}(\text{SiH}_3)^-$ , and  $(\text{H}_3\text{C})(\text{H}_3\text{Si})\text{C}=\text{Si}(\text{SiH}_3)\text{Li}\cdot 2\text{THF}$ , see the Supporting Information; b) J. A. Bohmann, F. Weinhold, T. C. Farrar, *J. Chem. Phys.* **1997**, *107*, 1173–1184.
- [30] For **2a**, see CCDC 1473315; for **2b**, see CCDC 1473316; for **2c**, see CCDC 1473317 as well as the Supporting Information. These data can be obtained free of charge from The Cambridge Crystallographic Data Centre via [www.ccdc.cam.ac.uk/data\\_request/cif](http://www.ccdc.cam.ac.uk/data_request/cif).
- [31] A. G. Brook, S. C. Nyburg, F. Abdesaken, B. Gutekunst, G. Gutekunst, R. Krishna, M. R. Kallury, Y. C. Poon, Y. M. Chang, W. N. Winnie, *J. Am. Chem. Soc.* **1982**, *104*, 5667–5672.
- [32] Y. Apeloig, M. Bendikov, M. Yuzefovich, M. Nakash, D. Bravo-Zhivotovskii, D. Bläser, R. Boese, *J. Am. Chem. Soc.* **1996**, *118*, 12228–12229.
- [33] N. Wiberg, G. Wagner, *Angew. Chem. Int. Ed. Engl.* **1983**, *22*, 1005–1006; *Angew. Chem.* **1983**, *95*, 1027–1028.

Received: April 14, 2016

Revised: April 25, 2016

Published online: July 28, 2016